HAMMER: Hairpin-based APOBEC3A-mediated mRNA editing reporter

Yanjun Chen[1], Christopher Mullally[1], Bojana Stefanovska[1,2], Reuben S. Harris[1,2,*]

[1] Department of Biochemistry and Structural Biology, University of Texas San Antonio, San Antonio, Texas, USA, 78229

[2] Howard Hughes Medical Institute, University of Texas San Antonio, San Antonio, Texas, USA, 78229

* To whom correspondence should be addressed. Email: rsh@uthscsa.edu

Manuscript Information: 61 character title, 200 word abstract, graphical abstract (below), 4,500 word main text (excluding references), Figs. 1-4, Supplementary Tables S1-S3, Supplementary Figs. S1-S2

Keywords: APOBEC3A (A3A); DNA cytosine-to-uracil deamination; DNA editing; live-cell reporter assay; RNA cytosine-to-uracil deamination; RNA editing; viral ribonucleotide reductase (RNR)

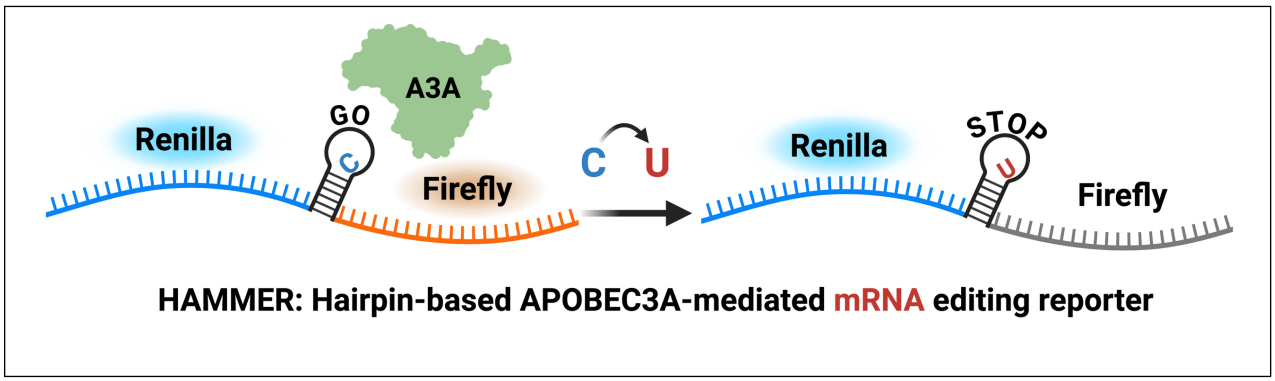

Abstract

APOBEC3A catalyzes cytosine-to-uracil deamination in single-stranded DNA and RNA. Physiologically, APOBEC3A functions in innate immunity and aberrant deamination is associated with cytosine mutations in enzymatically preferred YTCW substrate motifs in multiple cancers. Much less is known about the potential contribution of APOBEC3A-catalyzed RNA editing to virus and cancer evolution. Biosensors for quantification of APOBEC3A-mediated mRNA editing in living cells have yet to be developed. Here, we present HAMMER (hairpin-based APOBEC3A-mediated mRNA editing reporter), a rapid luminescence-based cellular assay for measuring RNA editing by APOBEC3A. HAMMER reports APOBEC3A activity as a reduction in the ratio of firefly to renilla luciferase activity. Briefly, tandem renilla and firefly luciferase open reading frames are separated by an optimal APOBEC3A hairpin substrate, in which C-to-U editing of a CGA motif yields a UGA stop codon thus preventing translation of the downstream firefly luciferase reporter and without impacting the upstream renilla reporter. HAMMER activation is dose-responsive, catalytic activity-dependent, and specific to human APOBEC3A. A panel of herpesviral ribonucleotide reductase constructs was used to show that direct inhibition of APOBEC3A results in a dose-responsive recovery of firefly luciferase expression. HAMMER is therefore a scalable and easy-to-use method for quantifying cellular APOBEC3A RNA editing activity and characterizing inhibitors.

Introduction

The seven human APOBEC3 enzymes (A3A-D and A3F-H) are generally thought to function as an overlapping innate immune barrier to endogenous and exogenous virus replication (reviewed by [1-5]). A variety of different viral families have been reported as substrates including retroviruses (HIV-1, HIV-2, HTLV), herpesviruses (EBV, KSHV, HSV-1), papillomaviruses (HPV), polyomaviruses (BKPyV, JCPyV), adenoviruses, parvoviruses, and others [1,3,6]. Key evidence for effector functions in antiviral immunity include potent virus restriction activity, copy number variability, genetic polymorphisms (positive selection), interferon-inducibility, and existence of an equally strong viral counterdefense mechanism [7]. As an example, human APOBEC3B (A3B)-mediated restriction of Epstein Barr virus (EBV) is counteracted by the large subunit of the viral ribonucleotide reductase (RNR) [8], and the copy numbers of human *A3B* and related *A3* genes vary between species [9], *A3B* itself is polymorphic within most species including humans [10-12], and *A3B* is regulated by infection and immunity signaling networks including (non)canonical NF-κB and interferon-α [13-17]. Despite sharing a common ancestor with present-day APOBEC3s, the related deaminases AID and APOBEC1 have different biological functions – AID as a genomic DNA deaminase in antibody gene diversification through somatic hypermutation and class switch recombination and APOBEC1 in mRNA editing (C6666 of the canonical *APOB* mRNA and many other coding and non-coding RNA substrates) [4].

APOBEC3A (A3A) is the most potent single-stranded (ss)DNA deaminase in humans [18-20]. A3A has a larger active site cavity than related human family members, which enables a broader range of substrates including normal cytosines in ssDNA or RNA as well as 5-methyl-C nucleobases in ssDNA [21-24]. Although A3A has been reported to restrict several of the viruses listed above, viral counterdefense mechanisms that selectively block this deaminase have yet to be described. Thus, unambiguous physiologic substrates have yet to be identified for this enzyme, although high relative activity and promiscuity are consistent with a more general role in foreign nucleic acid clearance [25,26]. The RNA cytosine deamination activity of A3A is not as well

characterized as its DNA editing activity. First discovered in human macrophages during M1 polarization and in monocytes in response to hypoxia and interferons, the RNA editing activity of A3A appears capable of impacting hundreds of sites including dozens at high efficiencies [27,28]. Many of the highest efficiency A3A RNA editing sites, including *SDHB* C136, are located in loop regions of hairpin structures [29,30], which is supported by structural studies with U-shaped ssDNA and hairpin DNA structures [21,23,31]. Interestingly, A3A signature edits have been reported in SARS-CoV-2 genomic RNA sequences suggesting a potential role for this deaminase in RNA virus mutation [32-34].

In contrast to beneficial roles in innate immune function, A3A can also be pathogenic in humans by contributing to cancer mutagenesis (reviewed by [5,35,36]). The broader substrate preference of A3A and the related enzyme A3B, YTCW and RTCW, respectively, is evident in nearly 70% of human tumor genomic DNA sequences and together are the largest sources of mutation in several cancer types including bladder and cervical [36-39]. C-to-T and C-to-G single base substitution mutations in TCW motifs comprise SBS2 and SBS13 mutation signatures in COSMIC [37]. Ectopic expression of A3A or A3B in mice increases rates of tumor formation and leads to APOBEC signature mutations [40-42]. A3A and A3B have also been shown to cause drug resistance mutations and associate with tumor metastases [43-45]. Several strategies are being developed to diagnose and treat A3A/B-positive tumors with the most straightforward being direct inhibition of the deaminases themselves [35,46,47].

However, a major hurdle to studying A3A function and evaluating candidate inhibitors is a lack of cell-based assays. This is in part due to toxicity of long-term ectopic over-expression of wildtype human A3A. One popular assay utilizes a cytosine base editing (CBE) complex to transiently deliver A3A to a ssDNA cytosine target in an R-loop, which can be read out as a restoration of fluorescence [48-52]. Another assay leverages highly sensitive digital droplet PCR technology to quantify A3A-exclusive RNA editing hotspots, such as hairpin loop cytosines in *SDHB* or *DDOST* mRNAs [30]. Here, we report the development of HAMMER – hairpin-based

A3A-mediated mRNA editing reporter – which utilizes a *DDOST*-derived hairpin substrate to provide a rapid luminescence-based readout of the RNA editing activity of A3A. The assay is highly specific to human A3A and, importantly, the luminescent read-out is directly proportional to the quantification of site-specific RNA editing by sequencing. HAMMER is therefore the first cell-based assay to report the mRNA editing of human A3A. HAMMER has advantages over other systems including the fact that A3A inhibition leads to a gain-of-signal readout (not a loss-of-signal), which facilitates inhibitor testing as evidenced here by surveying a panel of candidate A3A antagonists from herpesviruses.

Materials and Methods

Plasmids

The HAMMER *DDOST* Hairpin1 reporter was created using In-fusion Snap Assembly (Takara, 638948) to insert a synthetic gBlock (Integrated DNA Technologies) containing a renilla luciferase open reading frame (GenBank KF035113.1), a linker harboring a modified *DDOST* hairpin sequence and multiple restriction sites, and a firefly luciferase open reading frame (GenBank MT119956.1). The linker gBlock sequence is provided in **Table S1**. Additional HAMMER reporters were also constructed using In-fusion Snap Assembly by linearizing the *DDOST* Hairpin1 reporter linker region with HindIII (New England Biolabs, R3104L) and XbaI (New England Biolabs, R0145L) and inserting gBlocks containing candidate A3A hairpin substrates (gBlock sequences in **Table S1**). Stop1 and Linear1 control reporter plasmids were generated by site-directed mutagenesis of the *DDOST* Hairpin1 reporter construct (oligonucleotide sequences in **Table S2**).

pcDNA3.1 plasmids encoding untagged human A3A and A3A-E72A as well as C-terminal Myc-His tagged human A3A, A3B, A3Bctd, A3C, A3D, A3F, A3G, A3H-HapII, AID, and APOBEC1 deaminases have been described [19,53]. pcDNA4/TO plasmids encoding C-terminal FLAG-tagged RNRs and C-terminal eGFP-tagged A3A of *Homo sapiens* (human), *Macaca mulatta*

(rhesus macaque), and *Callithrix jacchus* (common marmoset) have also been reported [54,55]. GenBank accessions of the RNR constructs are described in **Table. S3**. Deaminase constructs correspond to the following GenBank accessions: *Homo sapiens* A3A (NM_145699.4), *Homo sapiens* A3B (NM_004900), *Homo sapiens* A3C (NM_014508.3), *Homo sapiens* A3D (NM_152426.4), *Homo sapiens* A3F (NM_145298.6), *Homo sapiens* A3G (NM_021822.4), *Homo sapiens* A3H-HapII (FJ376615.1); *Homo sapiens* AID (AICDA, NM_020661.4); *Homo sapiens* APOBEC1 (NM_001644.5); *Macaca mulatta* A3A (NM_001246231.1), and *Callithrix jacchus* A3A (NM_001301845.1). Expression plasmids for A1CF and RBM47 were obtained from AddGene (#112860 and #134607, respectively).

The DNA editing AMBER reporter and corresponding gRNA expression vector have been described [49]. The pCMV-Cas9n-BE4max construct was generated by site-directed mutagenesis to remove the rAPOBEC1 coding sequence [56,57]. Oligonucleotide sequences are provided in **Tables S2**.

Cell culture

HEK293T cells (ATCC CRL-3216) were maintained in RPMI-1640 medium (Thermo Fisher Scientific) supplemented with 10% (v/v) fetal bovine serum (Biowest) and 1% (v/v) penicillin-streptomycin (Gibco), at 37 °C with 5% CO_2.

HAMMER assay transfection and luciferase quantification

HEK293T cells were seeded in 12-well plates (Corning) and transfected at approximately 85% confluency. For standard experiments, 300 ng of HAMMER reporter plasmid, 200 ng of the indicated APOBEC expression plasmid, as well as 500ng of empty vector carrier DNA were co-transfected using 3 µL TransIT-LT1 (Mirus, #MIR 2300) per well, following the manufacturer's protocol.

At 4 hrs post-transfection, cells were trypsinized, and one-tenth of the cells from each well were transferred into a 96-well plate (Thermo Fisher Scientific, 65306) for luciferase measurements the next day. The remaining cells were replated into the original 12-well plate and collected the next day for immunoblotting and nucleic acid extraction (described below). Luciferase activity was measured 24 hrs post-transfection using the Dual-Glo Luciferase Assay System (Promega) according to the manufacturer's instructions, and luminescence was quantified using a Spark multimode microplate reader (Tecan).

Sanger sequencing of total DNA samples

For DNA analysis, transfected cells reseeded in 12-well plates were harvested at 24 hrs post-transfection. One-tenth of the cells from each well was pelleted and resuspended in QuickExtract™ DNA Extraction Solution (Biosearch Technologies, SS000035-D2) according to the manufacturer's protocol to obtain PCR-ready total DNA solution. 1 µL of processed solution was used as template for PCR amplification of the HAMMER reporter linker region using primers listed in **Table S2**. PCR products were size verified on a 1% agarose gel and purified using the Monarch® PCR & DNA Cleanup Kit (NEB, T1135). Purified amplicons were Sanger sequenced by Eurofins using primers listed in **Table S2**. Chromatograms received from Sanger sequencing were uploaded to EditR for peak quantification [58].

Reverse transcription and Sanger sequencing of cDNA samples

For RNA analysis, transfected cells in 12-well plates were harvested at 24 hrs post-transfection, and one-tenth of the cells from each well was pelleted for total RNA purification using the RNeasy Mini Kit (Qiagen, 74104). One microgram of purified RNA was reverse-transcribed using Transcriptor First Strand cDNA Synthesis Kit (Roche, #04897030001) according to the manufacturer's instructions. Purified cDNA was used as template for PCR amplification of the

HAMMER reporter linker region using primers listed in **Table S2**. PCR products were purified, sequenced, and quantified as described above.

Immunoblotting

For protein analysis, transfected cells in 12-well plates were harvested 24 hrs post-transfection, and about 80% of the cells were left after taken for DNA and RNA analysis described above. Cells were PBS washed, lysed in RIPA Buffer (Thermo Fisher Scientific, PI89900), and quantified by BCA assay (Thermo Fisher Scientific, 23225). Samples were then separated by 4-20% tris glycine polyacrylamide gels (Bio-Rad, 5671095) run for 90 minutes at 120V and transferred to PVDF-FL membrane (Millipore Sigma, IPFL00005). Following transfer, membrane was washed with 1X PBS with 0.1% Tween (PBST) before incubation in 1x casein blocking buffer (Sigma-Aldrich, C7594). Primary antibodies were diluted in 1x casein blocking buffer and incubated on membrane overnight at 4°C. Membrane was washed 3 times in 1X PBST and incubated with secondary antibodies diluted in 1x blocking buffer supplemented with 0.01% SDS. Following 1 hr of incubation at room temperature and 3 times of PBST wash, membrane was imaged on LiCor Odyssey Imager. Primary antibodies used were anti-A3A (5210-87-13 [59]; 1:1,000), anti-GFP (Cell Signal Technology, 2555S; 1:1,000), anti-Myc (Cell Signal Technology, 2278S; 1:1,000), anti-Flag (Sigma-Aldrich, F1804; 1:1,000), anti-Renilla luciferase (Abcam, EPR17792; 1:1,000), anti-β-Actin (Sigma Aldrich, A1978; 1:5,000), and anti-Tubulin (Sigma Aldrich, T5168; 1:5,000); Secondary antibodies used were anti-rabbit IRdye 800CW (LI-COR, 827-08365; 1:10,000) and anti-mouse IRdye 680LT (LI-COR, 925-68020; 1;10,000).

HAMMER experiments to test RNR inhibitory activity

HEK293T cells were seeded and transfected as described above. Specifically, cells were co-transfected with 300 ng HAMMER reporter plasmid, 200 ng A3A expression plasmid, 400 ng of the indicated RNR expression plasmid, and 100 ng empty vector carrier DNA using 3 µL

TransIT-LT1 per well. Sample processing and luciferase measurements were performed identically to the standard HAMMER workflow.

AMBER experiments to test RNR inhibitory activity

HEK293T cells were seeded in 12-well plates and transfected as described above. Cells were co-transfected with 300ng of AMBER reporter plasmid, 200 ng of Cas9n-BE4max plasmid, 100 ng of AMBER gRNA plasmid, 200ng of A3A expression plasmid, and 400 ng of the indicated RNR expression plasmid using 3.6 µL TransIT-LT1 per well. At 24 hrs, cells were trypsinized and suspended in 1 mL of PBS. An aliquot of 200 µL was used for flow cytometry to quantify mCherry and eGFP expression, and the remaining cells were pelleted for immunoblot analysis as described above.

Phylogenetic analysis of viral RNRs

Viral RNR amino-acid sequences (GenBank accessions listed in **Table S3**) were assembled in FASTA format and aligned with MAFFT (v7.490) [60]. The alignment was trimmed with trimAl (v1.4) to reduce poorly aligned and gap-rich regions. A maximum-likelihood phylogeny was inferred from the trimmed alignment using FastTree (v2.1.11) under the Jones–Taylor–Thornton (JTT) substitution model [61]. The resulting tree was midpoint-rooted (phytools in R) and visualized in R (v4.5.0) using ggtree (v4.0.1) [62].

Data analysis and figure generation

Illustrations of reporter constructs were generated with BioRender. Data analysis and figure generation were performed in GraphPad Prism. Reporter activation is calculated as the ratio of luminescence, Firefly/Renilla, and normalized to empty vector or catalytic mutant control where indicated. The student's T-test was used to assess differences in reporter activation, and Pearson correlation was used to determine correlation between reporter activation and DNA/RNA

editing. A threshold for significance was set at $P < 0.05$. Samples showing statistically significant differences relative to the indicated controls are annotated with *P*-values, and unlabeled comparisons did not reach the significance threshold.

Results

Construction of HAMMER – hairpin-based APOBEC3A-mediated mRNA editing reporter

The catalytic activity of A3A is strongly influenced by nucleic acid secondary structure. For instance, A3A exhibits a pronounced preference for cytosine nucleobases positioned on the 3' side of RNA and DNA hairpin loops [22,29,30,63-66]. This preference inspired the design of a series of dual-luciferase reporter plasmids to express in-frame renilla and firefly luciferase genes separated by a short linker sequence containing an editable hairpin (**Fig. 1A**). The initial Hairpin1 construct was based upon a naturally occurring hairpin in the *DDOST* transcript, because deamination of *DDOST* hairpin loop C558-to-U has been reported as a biomarker of A3A expression and activity [30]. However, in order to convert this hairpin into a viable reporter, the native *DDOST* hairpin had to be altered by swapping a single A-U base pair into U-A within the top of the hairpin stem (Hairpin1 in **Fig. 1A**). This change enabled a single C-to-U editing event within the hairpin loop CGA motif to yield a UGA stop codon, which completely blocks translation of the downstream firefly gene but does not alter translation of the upstream renilla gene (Stop1 in **Fig. 1A**). Thus, A3A-mediated deamination may be quantified by measuring the firefly-to-renilla luminescence ratio.

To test the signal-to-noise ratio of the Hairpin1 reporter, 293T cells were transfected with the Hairpin1 reporter in parallel with a Stop1 control, in which the target cytosine nucleobase in the loop is replaced with uracil to encode a constitutive stop codon (**Fig. 1A**). 293T cells were chosen due to no detectable endogenous *A3A* expression and high transient transfection efficiencies [59,67]. As expected, the Hairpin1 reporter expressed both renilla and firefly luciferase, whereas Edit1 only expressed renilla luciferase activity with firefly luciferase completely

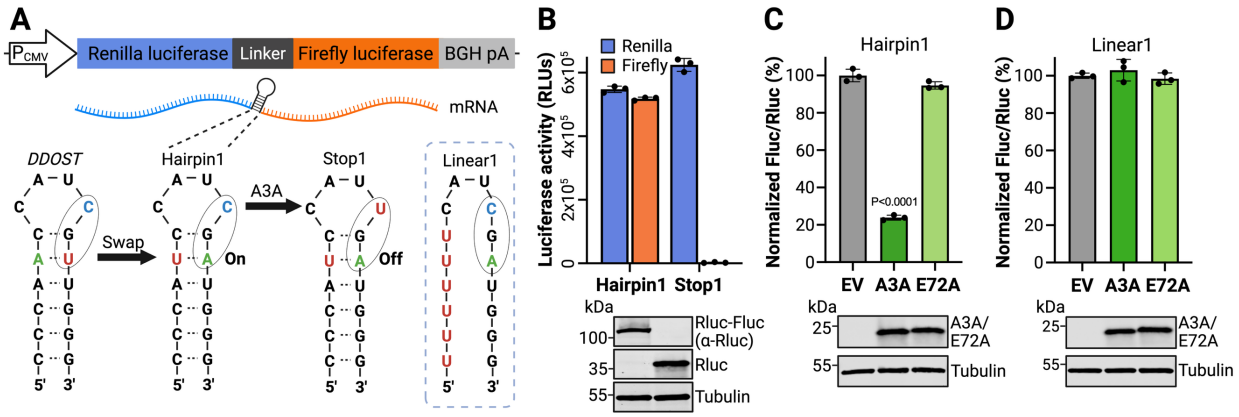

Fig. 1. Design and validation of the HAMMER reporter.

A, Schematic of the reporter construct with a constitutive CMV promoter, an upstream renilla luciferase (Rluc) gene, a linker region, and a downstream firefly luciferase (Fluc) gene. The linker region was engineered with a *DDOST-derived* hairpin (Hairpin1), an otherwise identical hairpin with a constitutive stop codon (Stop1), and a linear control (Linear1).
B, Luciferase activities of Hairpin1 and Stop1 reporters following transfection into 293T cells (RLU, relative luminescent units; mean ± SD of 3 reactions). Immunoblots shown below confirm expression of Rluc-FLuc chimeric protein by Hairpin1 and Rluc only by Stop1 with tubulin as a loading control.
C-D, Firefly-to-renilla luminescence ratios for Hairpin1 or Linear1 reporters co-transfected with an empty vector (EV), human A3A, or the human A3A-E72A catalytic mutant (mean ± SD of 3 reactions). Immunoblots shown below confirm expression of A3A and A3A-E72A with tubulin as a loading control.

suppressed by the engineered stop codon (**Fig. 1B**). Next, we tested whether the Hairpin1 reporter could detect A3A editing activity. Co-transfection of 293T cells with the Hairpin1 reporter and plasmids expressing wildtype A3A, catalytic mutant A3A-E72A, or an empty vector control showed that wildtype A3A reduces the firefly-to-renilla ratio by 80% (**Fig.1C**). In contrast, A3A-E72A had no significant effect (less than 3%). These results indicated that the Hairpin1 assay provides a direct read-out of A3A catalytic activity, most likely by RNA editing as designed.

To ask whether the hairpin structure is required for reporter function, a linear control construct was generated by changing the 5' side of the stem to uracil (Linear1 in **Fig.1A**). Importantly, the Linear1 construct preserves the UCG deamination target site, as well as two additional ribonucleobases upstream and all bases downstream. However, co-transfection of 293T cells with the Linear1 reporter and plasmids expressing wildtype A3A, catalytic mutant A3A-

E72A, or an empty vector control showed that wildtype A3A does not significantly alter the expression levels of the Linear1 reporter (**Fig. 1D**). Taken together, these results combined to indicate that the A3A-dependent diminution of firefly luciferase activity requires a hairpin structure as a substrate.

In addition to *DDOST1*, several additional RNA and DNA hairpin substrates have been reported for A3A [29,30,64] (**Fig. S1A**). Dual-luciferase reporter plasmids were designed for several of these hairpin substrates, such that single C-to-U editing events would yield a stop codon. To compare with the *DDOST*-derived Hairpin1 substrate, each of these constructs was co-transfected with A3A or A3A-E72A expression plasmids. Remarkably, the *DDOST*-derived Hairpin1 substrate was found to support the highest level of editing activity by A3A (**Fig. S1B**). *CYFIP1* C3222- and *SDHB* C136-based hairpin constructs also supported clear A3A editing activity, though both were significantly less than that observed with the *DDOST*-derived Hairpin1.

Although the enzymology of A3A on RNA hairpins has yet to be characterized comprehensively, studies on DNA hairpins have shown that A3A prefers substrates with longer stems, smaller loops (3-nt > 4-nt), and specific contexts (TTC loop over others) [63-66]. Guided by these principles, we engineered variants of the *DDOST* Hairpin1 with altered loop sizes, loop sequences, and extended stems (**Fig. S1C**). Contrary to expectations, all modifications reduced reporter activity and the original *DDOST*-based Hairpin1 substrate remained the most effective configuration (**Fig. S1D**). Given superior performance, the *DDOST* Hairpin1 reporter was used for all subsequent experiments, and the dual luciferase reporter system incorporating Hairpin1 is hereafter called the hairpin-based A3A-mediated mRNA editing reporter (HAMMER).

HAMMER reports A3A mRNA editing activity dose-responsively

We next evaluated whether HAMMER could report A3A activity in a dose-responsive manner. 293T cells were co-transfected with the HAMMER reporter and varying amounts of A3A or A3A-E72A expression constructs, and luciferase activity was measured 24 hrs post-

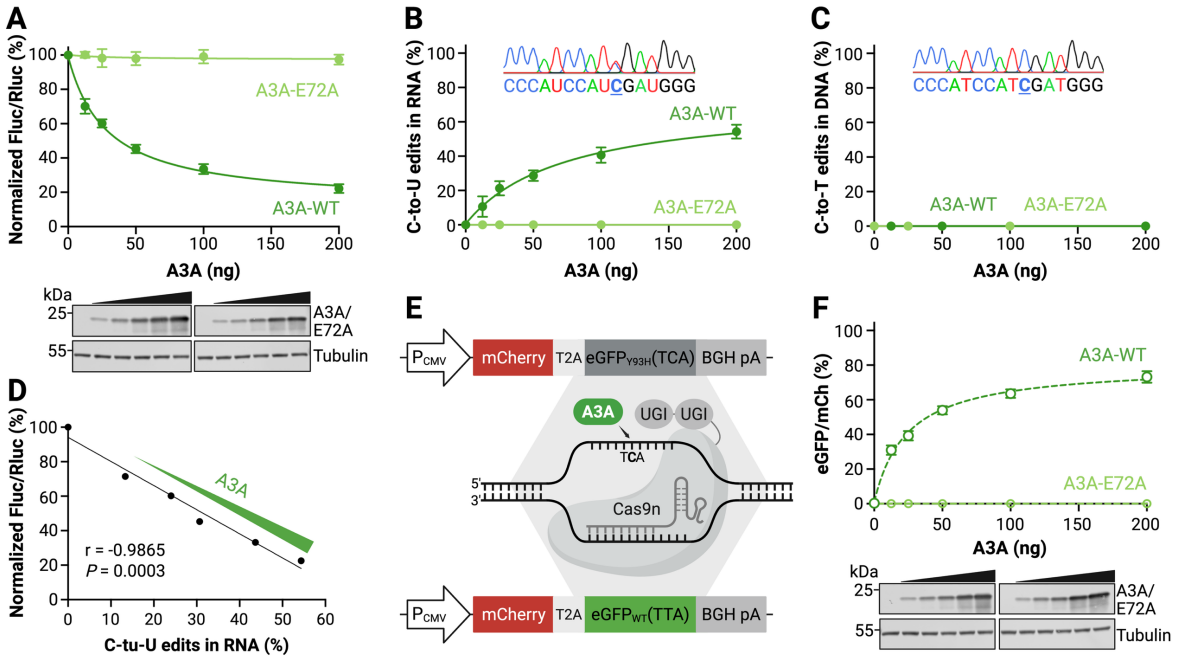

Fig. 2. HAMMER reports A3A activity dose-dependently and specifically on RNA.

A, Normalized firefly-to-renilla luminescence ratios of 293T cells co-transfected with the HAMMER reporter and increasing amounts of A3A or A3A-E72A plasmid. Data represent mean ± SD (n = 3), with some error bars smaller than the data points. Immunoblots shown below confirm dose-dependent expression of A3A and A3A-E72A.
B, Percentage of C-to-U edits in HAMMER reporter RNA following reverse transcription, PCR amplification, and Sanger sequencing. Data represent mean ± SD (n = 3), with some error bars smaller than the data points. A representative chromatogram from the 200 ng A3A expression condition is shown in the inset.
C, Percentage of C-to-T mutations detected in reporter DNA (DNA) PCR-amplified and Sanger-sequenced from the same reactions as panel B. Data represent mean ± SD (n = 3), with some error bars smaller than the data points. A representative chromatogram from the 200 ng A3A expression condition is shown in the inset.
D, Relationship between HAMMER luminescent readout and the percent mRNA C-to-U editing by A3A (2-fold dilution series starting at 200 ng; Pearson correlation coefficient (r) and *P*-value are indicated).
E, Schematic of the untethered DNA editing assay AMBER. An R-loop substrate created in eGFP using a gRNA/Cas9nickase-UGI complex can be edited by A3A to restore eGFP fluorescence.
F, eGFP fluorescence of 293T cells co-transfected with the AMBER reporter and increasing amounts of A3A or A3A-E72A plasmid. Data represent mean ± SD (n = 3), with some error bars smaller than the data points. Immunoblots shown below confirm dose-dependent expression of A3A and A3A-E72A.

transfection. Relative to the empty vector control, wildtype A3A decreased the firefly-to-renilla luminescence ratio in a clear dose-dependent fashion, and A3A-E72A did not produce a significant change in signal, even though the wildtype and catalytic mutant proteins were

expressed at similar levels in immunoblots (**Fig. 2A**). These data demonstrated that HAMMER quantitatively reports A3A activity across a wide range of expression levels.

As demonstrated previously, single-stranded DNA is the preferred, and often the exclusive, substrate of the seven human APOBEC3 family members [18,20,24,68]. Therefore, it is critical to determine whether the HAMMER signal originates from RNA editing rather than DNA deamination of the plasmid reporter. To directly address this possibility, total RNA and DNA were collected in parallel to the HAMMER assay. Sequencing results indicated that only the *DDOST*-derived Hairpin1 mRNA is edited by A3A, and that the corresponding DNA region is unaffected (**Fig. 2B-C**). Moreover, the luminescent readout of HAMMER (Fluc/Rluc) is directly proportional to the quantification of the C-to-U RNA editing frequencies by sequencing (**Fig. 2D**). These results confirm that HAMMER specifically reports RNA editing by A3A and is unlikely to be confounded by DNA deamination events.

As an additional control, parallel experiments were done in 293T cells using the same A3A expression constructs and a DNA C-to-T mutation reporter called AMBER (APOBEC-mediated base editing reporter) [48,49]. In this system, untethered A3A can access the target DNA cytosine in eGFP after exposure by a gRNA/Cas9nickase directed R-loop formation (assay schematic in **Fig. 2E**). Additionally, uracil excision repair is prevented by tethering two uracil DNA glycosylase inhibitory (Ugi) peptides to the C-terminal end of the Cas9nickase. As above, increasing amounts of transfected A3A but not A3A-E72A cause a dose-responsive change in reporter activity (here, increasing eGFP fluorescence; **Fig. 2F**). However, in contrast to HAMMER, all AMBER reporter activity is attributable to direct deamination of reporter DNA as established in the original reports [48,49].

HAMMER selectively detects human A3A RNA editing activity

Despite extensive structural homology and broadly conserved enzymatic function, APOBEC enzymes exhibit marked differences in catalytic activity, substrate preference, and

biological function [summarized in **Introduction** and reviewed in [1-4]]. All human *APOBEC3* family genes were derived from ancestral *AID* and *APOBEC1* sequences by multiple gene duplication and diversification events [11,69] (schematic of phylogenetic relationships in **Fig. 3A**). All nine of these human enzymes have shown DNA deamination activity in variety of contexts, but only APOBEC1, A3A, A3B, and A3G have been reported to edit RNA [27-29,70-75].

We therefore performed a head-to-head comparison of the nine active human APOBEC family members using the *DDOST*-derived HAMMER assay with the Hairpin1 substrate. First, 293T cells were co-transfected with HAMMER and expression plasmids encoding A3A, A3B, A3C, A3D, A3F, A3G, and A3H (**Fig. 3B**). Among >10 A3H haplotypes, HapII was used here because it is a common allele in the human population and the encoded enzyme is stable and catalytically active [76,77]. The C-terminal catalytic domain of A3B (A3Bctd) was also tested because it shares

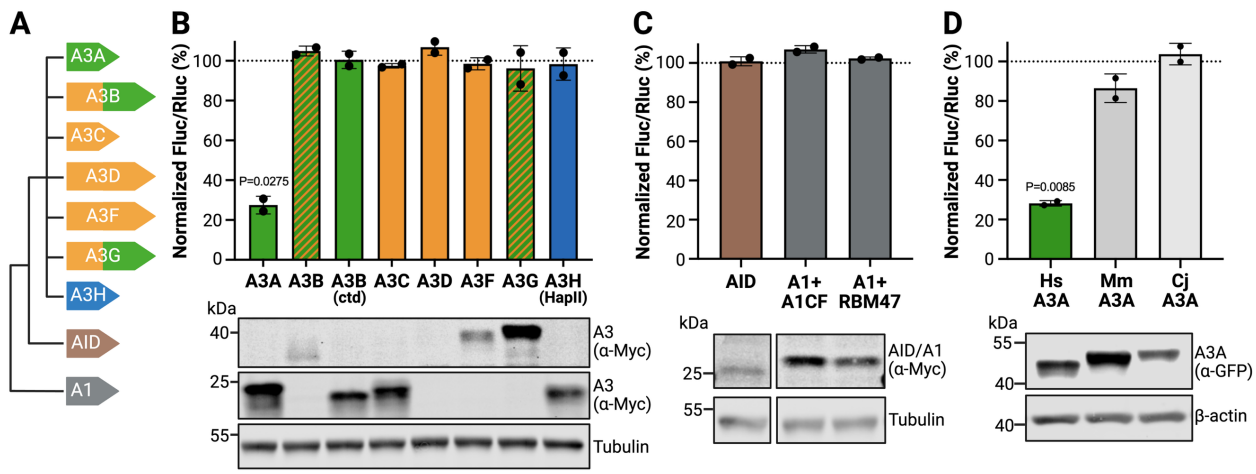

Fig. 3. HAMMER selectively detects RNA editing by human A3A.

A, Schematic of the nine catalytically active human APOBEC deaminase family members.
B, Firefly-to-renilla luminescence ratios for HAMMER performed with the indicated human APOBEC family member constructs (mean ± SD of 2 reactions normalized to vector control). Immunoblot of APOBEC expression (anti-Myc) with tubulin as a loading control.
C, Firefly-to-renilla luminescence ratios for HAMMER performed with AID, APOBEC1/A1CF, or APOBEC1/RBM47 (mean ± SD of 2 reactions normalized to vector control). Immunoblot of APOBEC expression (anti-Myc) with tubulin as a loading control (bands are from the same blot and reorganized for presentation to eliminate irrelevant lanes).
D, Firefly-to-renilla luminescence ratios for HAMMER performed with A3A orthologs from *Homo sapiens* (Hs), *Macaca mulatta* (Mm), and *Callithrix jacchus* (Cj) (mean ± SD of 2 reactions normalized to vector control). Immunoblot of deaminase expression (anti-GFP) with β-actin as a loading control.

89% amino acid identity (93% similarity) with A3A. As above, renilla and firefly luciferase activity was measured 24 hrs post-transfection. Among these constructs, only A3A edited the reporter as evidenced by a marked decrease in the firefly-to-renilla luminescence ratio (**Fig. 3B**). Even A3Bctd, which expressed to nearly the same extent as A3A, showed no detectable RNA editing activity. The double-domain enzymes, A3B, A3D, A3F, and A3G were not expressed as well but, despite repeated co-transfection experiments, these constructs showed no signs of activity in the HAMMER assay. Additional experiments also showed that neither human AID nor human APOBEC1 exhibit activity in HAMMER, even when the latter deaminase was co-expressed with physiologically relevant co-factors A1CF or RBM47 [78-80] (**Fig. 3C**). These results combined to indicate that HAMMER selectively reports human A3A activity.

As an additional test of specificity, HAMMER activity was compared for human A3A and orthologs from two non-human primate species – the Old World rhesus macaque (*Macaca mulatta*) and the New World common marmoset (*Callithrix jacchus*). These A3A proteins are 81% (88%) and 71% (82%) identical (similar) to the human enzyme. Interestingly, human A3A exhibited the strongest activity in HAMMER, the rhesus macaque A3A protein showed a modest effect, and the common marmoset A3A ortholog exhibited little to no activity (**Fig. 3D**). These experiments combine to underscore the specificity of the HAMMER assay for human A3A, because even some of its closest naturally occurring orthologs (A3Bctd) and homologs (MmA3A and CjA3A) are unable to approach its robust Hairpin1 RNA editing activity.

HAMMER identifies herpesvirus RNRs that inhibit A3A

Prior studies have shown that the EBV large RNR subunit BORF2 directly binds to A3Bctd, inhibits its catalytic activity, and triggers its accumulation into perinuclear aggregates [8,81,82]. As noted above, human A3A is 89% identical/93% similar to human A3Bctd, and it can also be bound by EBV BORF2 and relocalized into aggregates [54,82]. Therefore, as a first proof-of-concept, we sought to test whether EBV BORF2 and related herpesviral RNR large subunits have

the capacity to inhibit A3A-catalyzed RNA editing using HAMMER. For comparison, all RNR constructs were also tested in parallel for inhibition of A3A-catalyzed DNA editing using an untethered version of AMBER (schematic in **Fig. 2E**). The herpesvirus large RNR subunits surveyed here are derived from the human α-herpesvirus HSV-1 and from human and Old and New World primate γ-herpesviruses from the lymphocryptovirus and rhadinoherpesvirus groups (phylogenetic relationships in **Fig. 4A**).

First, titration experiments were performed to ask whether BORF2 inhibits A3A-catalyzed HAMMER read-out dose-responsively. As above, A3A caused a 60% reduction in firefly luciferase in HAMMER and, interestingly, BORF2 restored luminescence dose-responsively to near wildtype levels at the highest transfected amounts (**Fig. 4B**). In a parallel experiment, A3A caused a 30% restoration of eGFP fluorescence in AMBER, and BORF2 inhibited this DNA editing activity dose responsively with near-complete inhibition at highest expression levels, consistent with prior reports [49,83] (**Fig. 4C**). A strong correlation between RNA and DNA editing inhibition indicated that EBV BORF2 is capable of inhibiting both of these human A3A activities (**Fig. S2**).

Second, the large RNR subunit of HSV-1 (ICP6) was tested in comparison with that of lymphocryptovirus EBV (BORF2) and the rhadinoherpesvirus KSHV (ORF61). Relative to EBV BORF2, which inhibited A3A strongly, the large RNR subunits of HSV-1 and KSHV appeared to have intermediate inhibitory activities (**Fig. 4D-E**). Third, RNRs from several New World primates were tested and none of these proteins appeared to inhibit either the RNA or the DNA editing activity of human A3A (**Fig. 4D-E**). Fourth and in striking contrast to the New World viral RNRs, the large RNR subunits from several Old World primates were tested and, surprisingly, all of them inhibited both RNA and DNA editing activity of human A3A (**Fig. 4D-E**). Most remarkably, two of these Old World viral RNRs, the large RNR subunits from the lymphocryptovirus McHV4 and the

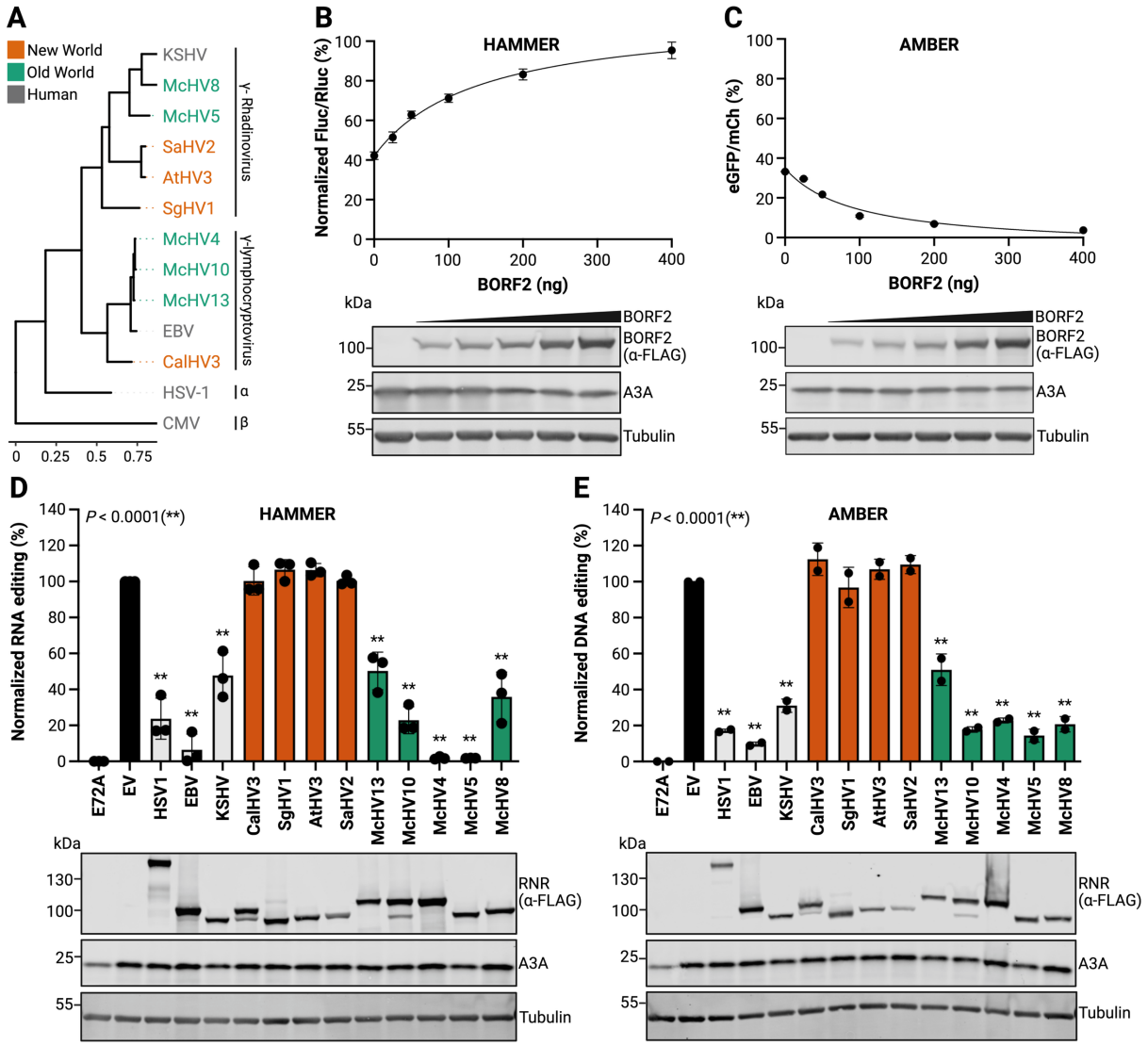

Fig. 4. HAMMER identifies herpes virus RNRs that inhibit A3A activity

A, Phylogenetic tree of viral RNR family members tested in HAMMER and AMBER assays (the β-herpesvirus human CMV is included as a more distantly related outgroup).
B-C, HAMMER and AMBER results, respectively, for 293T cells co-transfected with each reporter, 200 ng A3A, and the indicated amounts of an EBV BORF2 construct. Data represent the mean ± SD of technical triplicate experiments, with some error bars smaller than the data points. Immunoblots showing A3A and BORF2 expression with tubulin as a loading control.
D-E, HAMMER and AMBER results, respectively, for 293T cells co-transfected with each reporter, 200 ng A3A, and the indicated viral RNR constructs. HAMMER activity was quantified by normalizing firefly-to-renilla luminescence ratios to EV control (100%) and E72A control (0%). AMBER activity was quantified by normalizing eGFP+ to mCherry+ cell count ratios to EV control (100%) and E72A control (as 0%). Data represent mean ± SD of three (HAMMER) or two (AMBER) experiments. Immunoblots show A3A and RNR expression with tubulin as a loading control.

rhadinoherpesvirus McHV5 proved to be as potent as EBV BORF2 at blocking A3A activity. These

results demonstrate that HAMMER can be used to identify candidate A3A inhibitors by virtue of clear gain-of-signal readouts.

Discussion

Here, we present HAMMER (hairpin-based APOBEC3A-mediated mRNA editing reporter) for quantification of the RNA editing activity of human A3A in living cells. A3A dose-responsively edits a *DDOST*-derived hairpin substrate (Hairpin1), which yields a stop codon preventing expression of the downstream firefly luciferase reporter and leaving the upstream renilla luciferase reporter unaffected. Thus, RNA editing by A3A becomes a simple metric of the ratio of firefly to renilla luminescence values. Importantly, sequencing showed that human A3A specifically edits the reporter mRNA and does not significantly alter the corresponding DNA sequence in the transfected HAMMER construct. HAMMER is highly specific to RNA editing by human A3A, because no other active human polynucleotide deaminase exhibits activity in this assay. Even human A3Bctd (93% similar to human A3A) and the textbook RNA editing enzyme APOBEC1 show no activity in HAMMER. However, the 88% similar rhesus macaque A3A protein exhibits modest activity in HAMMER suggesting that relatively small amino acid and structural differences are likely to account for the optimal activity of human A3A with this reporter system.

We anticipate that HAMMER will become a valuable addition to the toolbox of cellular assays used to study A3A function in biology and disease [84]. As the only cell-based RNA-centric assay to-date, it will complement DNA-based assays such as AMBER used here and others that similarly leverage tethered or untethered cytosine base editing technologies [48-52,85,86]. As outlined in **Introduction**, A3A has been reported to interact with a broad number of DNA and RNA-based viruses. However, a true physiological substrate for A3A remains debatable because a key hallmark of a virus restriction factor has yet to be satisfied – *i.e.*, a virus has yet to be found that encodes an equally potent A3A neutralization mechanism. It is therefore possible that HAMMER could be used to screen for such a factor and, minimally, once discovered to help

characterize the underlying molecular mechanism. Here, as proof-of-concept, we tested a panel of herpesviral RNR large subunits against human A3A. Although human and Old World monkey A3B enzymes are clearly physiological targets of several of these viral RNRs [54], the high degree of similarity between the C-terminal catalytic domain of human A3B and human A3A suggested that some of the viral RNRs might also inhibit A3A through molecular mimicry [54]. Indeed, in addition to the RNR large subunits from several human viruses (EBV, KSHV, and HSV-1), several Old World primate viral RNR large subunits were also able to inhibit human A3A activity in HAMMER. Notably, the RNR large subunits from McHV4 and McHV5 were as potent as EBV BORF2 at blocking the mRNA editing activity of human A3A. Likewise, HAMMER is also envisaged to be useful for identifying and characterizing small molecules that impact A3A function in cells.

Acknowledgments

We are grateful to Michael Carpenter, Allen York, and other lab members for thoughtful feedback. R.S.H. is an Investigator of the Howard Hughes Medical Institute and the Ewing Halsell President's Council Distinguished Chair at University of Texas San Antonio.

Supplementary Data

Supplementary Data are available at NAR Online.

Conflicts of Interest

The authors declare no competing interests.

Funding

This work was supported by National Cancer Institute P01-CA234228 and P50-CA247749 and a Recruitment of Established Investigators Award from the Cancer Prevention and Research

Institute of Texas (CPRIT RR220053). Partial salary support for C.M. was provided by the South Texas Medical Scientist Training Program (NIGMS T32-GM113896 and T32-GM145432) and the Epigenetics, DNA Repair, Genomics (EDGe) Training Program (NCI T32-CA279363).

Data Availability

All data are reported in the main manuscript or supplementary material.

Author Contributions

Conceptualization: All authors. Methodology: YC, CM, RSH. Investigation: YC, BS, CM. Visualization: All authors. Funding acquisition: All authors. Simulations and Data Analysis: All authors. Project administration: RSH. Supervision: RSH. Writing – original draft: All authors. Writing – review & editing: All authors.

References

1. Harris, R.S. and Dudley, J.P. (2015) APOBECs and virus restriction. *Virology*, **479-480C**, 131-145.
2. Hou, S., Lee, J.M., Myint, W., Matsuo, H., Kurt Yilmaz, N. and Schiffer, C.A. (2021) Structural basis of substrate specificity in human cytidine deaminase family APOBEC3s. *J Biol Chem*, **297**, 100909.
3. Cheng, A.Z., Moraes, S.N., Shaban, N.M., Fanunza, E., Bierle, C.J., Southern, P.J., Bresnahan, W.A., Rice, S.A. and Harris, R.S. (2021) APOBECs and herpesviruses. *Viruses*, **13**.
4. Siriwardena, S.U., Chen, K. and Bhagwat, A.S. (2016) Functions and malfunctions of mammalian DNA-cytosine deaminases. *Chem Rev*, **116**, 12688-12710.
5. Green, A.M. and Weitzman, M.D. (2019) The spectrum of APOBEC3 activity: From anti-viral agents to anti-cancer opportunities. *DNA Repair (Amst)*, **83**, 102700.

6. Poulain, F., Lejeune, N., Willemart, K. and Gillet, N.A. (2020) Footprint of the host restriction factors APOBEC3 on the genome of human viruses. *PLoS Pathog*, **16**, e1008718.
7. Harris, R.S., Hultquist, J.F. and Evans, D.T. (2012) The restriction factors of human immunodeficiency virus. *J Biol Chem*, **287**, 40875-40883.
8. Cheng, A.Z., Yockteng-Melgar, J., Jarvis, M.C., Malik-Soni, N., Borozan, I., Carpenter, M.A., McCann, J.L., Ebrahimi, D., Shaban, N.M., Marcon, E. *et al.* (2019) Epstein-Barr virus BORF2 inhibits cellular APOBEC3B to preserve viral genome integrity. *Nature microbiology*, **4**, 78-88.
9. LaRue, R.S., Jónsson, S.R., Silverstein, K.A.T., Lajoie, M., Bertrand, D., El-Mabrouk, N., Hötzel, I., Andrésdóttir, V., Smith, T.P.L. and Harris, R.S. (2008) The artiodactyl APOBEC3 innate immune repertoire shows evidence for a multi-functional domain organization that existed in the ancestor of placental mammals. *BMC Mol Biol*, **9**, 104.
10. Kidd, J.M., Newman, T.L., Tuzun, E., Kaul, R. and Eichler, E.E. (2007) Population stratification of a common APOBEC gene deletion polymorphism. *PLoS Genet*, **3**, e63.
11. Uriu, K., Kosugi, Y., Suzuki, N., Ito, J. and Sato, K. (2021) Elucidation of the complicated scenario of primate APOBEC3 gene evolution. *J Virol*, **95**.
12. Ito, J., Gifford, R.J. and Sato, K. (2020) Retroviruses drive the rapid evolution of mammalian APOBEC3 genes. *Proc Natl Acad Sci U S A*, **117**, 610-618.
13. Roelofs, P.A., Goh, C.Y., Chua, B.H., Jarvis, M.C., Stewart, T.A., McCann, J.L., McDougle, R.M., Carpenter, M.A., Martens, J.W., Span, P.N. *et al.* (2020) Characterization of the mechanism by which the RB/E2F pathway controls expression of the cancer genomic DNA deaminase APOBEC3B. *Elife*, **9**.
14. Maruyama, W., Shirakawa, K., Matsui, H., Matsumoto, T., Yamazaki, H., Sarca, A.D., Kazuma, Y., Kobayashi, M., Shindo, K. and Takaori-Kondo, A. (2016) Classical NF-kappaB pathway is responsible for APOBEC3B expression in cancer cells. *Biochem Biophys Res Commun*, **478**, 1466-1471.

15.Leonard, B., McCann, J.L., Starrett, G.J., Kosyakovsky, L., Luengas, E.M., Molan, A.M., Burns, M.B., McDougle, R.M., Parker, P.J., Brown, W.L. *et al.* (2015) The PKC/NF-kappaB signaling pathway induces APOBEC3B expression in multiple human cancers. *Cancer Res*, **75**, 4538-4547.

16. Kanu, N., Cerone, M.A., Goh, G., Zalmas, L.P., Bartkova, J., Dietzen, M., McGranahan, N., Rogers, R., Law, E.K., Gromova, I. *et al.* (2016) DNA replication stress mediates APOBEC3 family mutagenesis in breast cancer. *Genome Biol*, **17**, 185.

17. Oh, S., Bournique, E., Bowen, D., Jalili, P., Sanchez, A., Ward, I., Dananberg, A., Manjunath, L., Tran, G.P., Semler, B.L. *et al.* (2021) Genotoxic stress and viral infection induce transient expression of APOBEC3A and pro-inflammatory genes through two distinct pathways. *Nat Commun*, **12**, 4917.

18. Ito, F., Fu, Y., Kao, S.A., Yang, H. and Chen, X.S. (2017) Family-wide comparative analysis of cytidine and methylcytidine deamination by eleven human APOBEC proteins. *J Mol Biol*, **429**, 1787-1799.

19.Carpenter, M.A., Li, M., Rathore, A., Lackey, L., Law, E.K., Land, A.M., Leonard, B., Shandilya, S.M., Bohn, M.F., Schiffer, C.A. *et al.* (2012) Methylcytosine and normal cytosine deamination by the foreign DNA restriction enzyme APOBEC3A. *J Biol Chem*, **287**, 34801-34808.

20. Schutsky, E.K., Nabel, C.S., Davis, A.K.F., DeNizio, J.E. and Kohli, R.M. (2017) APOBEC3A efficiently deaminates methylated, but not TET-oxidized, cytosine bases in DNA. *Nucleic Acids Res*, **45**, 7655-7665.

21. Kouno, T., Silvas, T.V., Hilbert, B.J., Shandilya, S.M.D., Bohn, M.F., Kelch, B.A., Royer, W.E., Somasundaran, M., Kurt Yilmaz, N., Matsuo, H. *et al.* (2017) Crystal structure of APOBEC3A bound to single-stranded DNA reveals structural basis for cytidine deamination and specificity. *Nat Commun*, **8**, 15024.

22. Silvas, T.V., Hou, S., Myint, W., Nalivaika, E., Somasundaran, M., Kelch, B.A., Matsuo, H.,

Kurt Yilmaz, N. and Schiffer, C.A. (2018) Substrate sequence selectivity of APOBEC3A implicates intra-DNA interactions. *Sci Rep*, **8**, 7511.

23. Shi, K., Carpenter, M.A., Banerjee, S., Shaban, N.M., Kurahashi, K., Salamango, D.J., McCann, J.L., Starrett, G.J., Duffy, J.V., Demir, O. *et al.* (2017) Structural basis for targeted DNA cytosine deamination and mutagenesis by APOBEC3A and APOBEC3B. *Nat Struct Mol Biol*, **24**, 131-139.
24. Wyllie, M.K., Morris, C.K., Moeller, N.H., Schares, H.A.M., Moorthy, R., Belica, C.A., Grillo, M.J., Demir, O., Ayoub, A.M., Carpenter, M.A. *et al.* (2025) The Impact of sugar conformation on the single-stranded DNA selectivity of APOBEC3A and APOBEC3B enzymes. *ACS Chem Biol*, **20**, 117-127.
25. Stenglein, M.D., Burns, M.B., Li, M., Lengyel, J. and Harris, R.S. (2010) APOBEC3 proteins mediate the clearance of foreign DNA from human cells. *Nat Struct Mol Biol*, **17**, 222-229.
26. Suspène, R., Aynaud, M.M., Guetard, D., Henry, M., Eckhoff, G., Marchio, A., Pineau, P., Dejean, A., Vartanian, J.P. and Wain-Hobson, S. (2011) Somatic hypermutation of human mitochondrial and nuclear DNA by APOBEC3 cytidine deaminases, a pathway for DNA catabolism. *Proc Natl Acad Sci U S A*, **108**, 4858-4863.
27. Sharma, S., Patnaik, S.K., Taggart, R.T., Kannisto, E.D., Enriquez, S.M., Gollnick, P. and Baysal, B.E. (2015) APOBEC3A cytidine deaminase induces RNA editing in monocytes and macrophages. *Nat Commun*, **6**, 6881.
28. Sharma, S., Patnaik, S.K., Kemer, Z. and Baysal, B.E. (2017) Transient overexpression of exogenous APOBEC3A causes C-to-U RNA editing of thousands of genes. *RNA biology*, **14**, 603-610.
29. Sharma, S. and Baysal, B.E. (2017) Stem-loop structure preference for site-specific RNA editing by APOBEC3A and APOBEC3G. *PeerJ*, **5**, e4136.
30. Jalili, P., Bowen, D., Langenbucher, A., Park, S., Aguirre, K., Corcoran, R.B., Fleischman, A.G., Lawrence, M.S., Zou, L. and Buisson, R. (2020) Quantification of ongoing

APOBEC3A activity in tumor cells by monitoring RNA editing at hotspots. *Nat Commun*, **11**, 2971.

31. Harjes, S., Kurup, H.M., Rieffer, A.E., Bayarjargal, M., Filitcheva, J., Su, Y., Hale, T.K., Filichev, V.V., Harjes, E., Harris, R.S. *et al.* (2023) Structure-guided inhibition of the cancer DNA-mutating enzyme APOBEC3A. *Nat Commun*, **14**, 6382.

32. Begum, M.M., Bokani, A., Rajib, S.A., Soleimanpour, M., Maeda, Y., Yoshimura, K., Satou, Y., Ebrahimi, D. and Ikeda, T. (2024) Potential role of APOBEC3 family proteins in SARS-CoV-2 replication. *Viruses*, **16**.

33. Kim, K., Calabrese, P., Wang, S., Qin, C., Rao, Y., Feng, P. and Chen, X.S. (2022) The roles of APOBEC-mediated RNA editing in SARS-CoV-2 mutations, replication and fitness. *Sci Rep*, **12**, 14972.

34. Nakata, Y., Ode, H., Kubota, M., Kasahara, T., Matsuoka, K., Sugimoto, A., Imahashi, M., Yokomaku, Y. and Iwatani, Y. (2023) Cellular APOBEC3A deaminase drives mutations in the SARS-CoV-2 genome. *Nucleic Acids Res*, **51**, 783-795.

35. Petljak, M., Green, A.M., Maciejowski, J. and Weitzman, M.D. (2022) Addressing the benefits of inhibiting APOBEC3-dependent mutagenesis in cancer. *Nat Genet*, **54**, 1599-1608.

36. Swanton, C., McGranahan, N., Starrett, G.J. and Harris, R.S. (2015) APOBEC enzymes: mutagenic fuel for cancer evolution and heterogeneity. *Cancer Discov*, **5**, 704-712.

37. Alexandrov, L.B., Kim, J., Haradhvala, N.J., Huang, M.N., Tian Ng, A.W., Wu, Y., Boot, A., Covington, K.R., Gordenin, D.A., Bergstrom, E.N. *et al.* (2020) The repertoire of mutational signatures in human cancer. *Nature*, **578**, 94-101.

38. Roberts, S.A. and Gordenin, D.A. (2014) Hypermutation in human cancer genomes: footprints and mechanisms. *Nature Reviews*, **14**, 786-800.

39. Burns, M.B., Temiz, N.A. and Harris, R.S. (2013) Evidence for APOBEC3B mutagenesis in multiple human cancers. *Nat Genet*, **45**, 977-983.

40. Law, E.K., Levin-Klein, R., Jarvis, M.C., Kim, H., Argyris, P.P., Carpenter, M.A., Starrett, G.J.,

Temiz, N.A., Larson, L.K., Durfee, C. *et al.* (2020) APOBEC3A catalyzes mutation and drives carcinogenesis in vivo. *J Exp Med*, **217**.

41. Naumann, J.A., Argyris, P.P., Carpenter, M.A., Gupta, H.B., Chen, Y., Temiz, N.A., Zhou, Y., Durfee, C., Proehl, J., Koniar, B.L. *et al.* (2023) DNA deamination is required for human APOBEC3A-driven hepatocellular carcinoma *in vivo*. *International Journal of Molecular Sciences*, **24**.
42. Durfee, C., Temiz, N.A., Levin-Klein, R., Argyris, P.P., Alsoe, L., Carracedo, S., Alonso de la Vega, A., Proehl, J., Holzhauer, A.M., Seeman, Z.J. *et al.* (2023) Human APOBEC3B promotes tumor development *in vivo* including signature mutations and metastases. *Cell Rep Med*, **4**, 101211.
43. Law, E.K., Sieuwerts, A.M., LaPara, K., Leonard, B., Starrett, G.J., Molan, A.M., Temiz, N.A., Vogel, R.I., Meijer-van Gelder, M.E., Sweep, F.C. *et al.* (2016) The DNA cytosine deaminase APOBEC3B promotes tamoxifen resistance in ER-positive breast cancer. *Sci Adv*, **2**, e1601737.
44. Gupta, A., Gazzo, A., Selenica, P., Safonov, A., Pareja, F., da Silva, E.M., Brown, D.N., Shao, H., Zhu, Y., Patel, J. *et al.* (2025) APOBEC3 mutagenesis drives therapy resistance in breast cancer. *Nat Genet*.
45. Isozaki, H., Sakhtemani, R., Abbasi, A., Nikpour, N., Stanzione, M., Oh, S., Langenbucher, A., Monroe, S., Su, W., Cabanos, H.F. *et al.* (2023) Therapy-induced APOBEC3A drives evolution of persistent cancer cells. *Nature*, **620**, 393-401.
46. Harris, R.S. (2013) Cancer mutation signatures, DNA damage mechanisms, and potential clinical implications. *Genome Medicine*, **5**, 87.
47. Roelofs, P.A., Martens, J.W.M., Harris, R.S. and Span, P.N. (2023) Clinical implications of APOBEC3-mediated mutagenesis in breast cancer. *Clin Cancer Res*, **29**, 1658-1669.
48. St. Martin, A., Salamango, D.J., Serebrenik, A.A., Shaban, N.M., Brown, W.L. and Harris, R.S. (2019) A panel of eGFP reporters for single base editing by APOBEC-Cas9 editosome

complexes. *Sci Rep*, **9**, 497.

49. Rieffer, A.E., Chen, Y., Salamango, D.J., Moraes, S.N. and Harris, R.S. (2023) APOBEC reporter systems for evaluating diNucleotide editing levels. *CRISPR J*, **6**, 430-446.
50. Gu, S., Bodai, Z., Anderson, R.A., So, H.Y.A., Cowan, Q.T. and Komor, A.C. (2025) Elucidating the genetic mechanisms governing cytosine base editing outcomes through CRISPRi screens. *Nat Commun*, **16**, 4685.
51. Standage-Beier, K., Tekel, S.J., Brookhouser, N., Schwarz, G., Nguyen, T., Wang, X. and Brafman, D.A. (2019) A transient reporter for editing enrichment (TREE) in human cells. *Nucleic Acids Res*, **47**, e120.
52. Coelho, M.A., Li, S., Pane, L.S., Firth, M., Ciotta, G., Wrigley, J.D., Cuomo, M.E., Maresca, M. and Taylor, B.J.M. (2018) BE-FLARE: a fluorescent reporter of base editing activity reveals editing characteristics of APOBEC3A and APOBEC3B. *BMC biology*, **16**, 150.
53. Hultquist, J.F., Lengyel, J.A., Refsland, E.W., LaRue, R.S., Lackey, L., Brown, W.L. and Harris, R.S. (2011) Human and rhesus APOBEC3D, APOBEC3F, APOBEC3G, and APOBEC3H demonstrate a conserved capacity to restrict Vif-deficient HIV-1. *J Virol*, **85**, 11220-11234.
54. Moraes, S.N., Becker, J.T., Moghadasi, S.A., Shaban, N.M., Auerbach, A.A., Cheng, A.Z. and Harris, R.S. (2022) Evidence linking APOBEC3B genesis and evolution of innate immune antagonism by gamma-herpesvirus ribonucleotide reductases. *Elife*, **11**.
55. Auerbach, A.A., Becker, J.T., Moraes, S.N., Moghadasi, S.A., Duda, J.M., Salamango, D.J. and Harris, R.S. (2022) Ancestral APOBEC3B nuclear localization is maintained in humans and apes and altered in most other Old World primate species. *mSphere*, **7**, e0045122.
56. Koblan, L.W., Doman, J.L., Wilson, C., Levy, J.M., Tay, T., Newby, G.A., Maianti, J.P., Raguram, A. and Liu, D.R. (2018) Improving cytidine and adenine base editors by expression optimization and ancestral reconstruction. *Nat Biotechnol*, **36**, 843-846.
57. Komor, A.C., Zhao, K.T., Packer, M.S., Gaudelli, N.M., Waterbury, A.L., Koblan, L.W., Kim,

Y.B., Badran, A.H. and Liu, D.R. (2017) Improved base excision repair inhibition and bacteriophage Mu Gam protein yields C:G-to-T:A base editors with higher efficiency and product purity. *Sci Adv*, **3**, eaao4774.

58. Kluesner, M.G., Nedveck, D.A., Lahr, W.S., Garbe, J.R., Abrahante, J.E., Webber, B.R. and Moriarity, B.S. (2018) EditR: A Method to Quantify Base Editing from Sanger Sequencing. *CRISPR J*, **1**, 239-250.
59. Brown, W.L., Law, E.K., Argyris, P.P., Carpenter, M.A., Levin-Klein, R., Ranum, A.N., Molan, A.M., Forster, C.L., Anderson, B.D., Lackey, L. *et al.* (2019) A rabbit monoclonal antibody against the antiviral and cancer genomic DNA mutating enzyme APOBEC3B. *Antibodies (Basel)*, **8**.
60. Katoh, K. and Standley, D.M. (2013) MAFFT multiple sequence alignment software version 7: improvements in performance and usability. *Mol Biol Evol*, **30**, 772-780.
61. Price, M.N., Dehal, P.S. and Arkin, A.P. (2010) FastTree 2--approximately maximum-likelihood trees for large alignments. *PloS One*, **5**, e9490.
62. Yu, G. (2020) Using ggtree to visualize data on tree-like structures. *Current protocols in bioinformatics* **69**, e96.
63. Langenbucher, A., Bowen, D., Sakhtemani, R., Bournique, E., Wise, J.F., Zou, L., Bhagwat, A.S., Buisson, R. and Lawrence, M.S. (2021) An extended APOBEC3A mutation signature in cancer. *Nat Commun*, **12**, 1602.
64. Buisson, R., Langenbucher, A., Bowen, D., Kwan, E.E., Benes, C.H., Zou, L. and Lawrence, M.S. (2019) Passenger hotspot mutations in cancer driven by APOBEC3A and mesoscale genomic features. *Science*, **364**.
65. Butt, Y., Sakhtemani, R., Mohamad-Ramshan, R., Lawrence, M.S. and Bhagwat, A.S. (2024) Distinguishing preferences of human APOBEC3A and APOBEC3B for cytosines in hairpin loops, and reflection of these preferences in APOBEC-signature cancer genome mutations. *Nat Commun*, **15**, 2369.

66. Sanchez, A., Ortega, P., Sakhtemani, R., Manjunath, L., Oh, S., Bournique, E., Becker, A., Kim, K., Durfee, C., Temiz, N.A. *et al.* (2024) Mesoscale DNA features impact APOBEC3A and APOBEC3B deaminase activity and shape tumor mutational landscapes. *Nat Commun*, **15**, 2370.

67. Carpenter, M.A., Temiz, N.A., Ibrahim, M.A., Jarvis, M.C., Brown, M.R., Argyris, P.P., Brown, W.L., Starrett, G.J., Yee, D. and Harris, R.S. (2023) Mutational impact of APOBEC3A and APOBEC3B in a human cell line and comparisons to breast cancer. *PLoS Genet*, **19**, e1011043.

68. McCann, J.L., Cristini, A., Law, E.K., Lee, S.Y., Tellier, M., Carpenter, M.A., Beghe, C., Kim, J.J., Sanchez, A., Jarvis, M.C. *et al.* (2023) APOBEC3B regulates R-loops and promotes transcription-associated mutagenesis in cancer. *Nat Genet*, **55**, 1721-1734.

69. Harris, R.S. and Liddament, M.T. (2004) Retroviral restriction by APOBEC proteins. *Nat Rev Immunol*, **4**, 868-877.

70. Smith, H.C. (2017) RNA binding to APOBEC deaminases; Not simply a substrate for C to U editing. *RNA Biology*, **14**, 1153-1165.

71. Alqassim, E.Y., Sharma, S., Khan, A., Emmons, T.R., Cortes Gomez, E., Alahmari, A., Singel, K.L., Mark, J., Davidson, B.A., Robert McGray, A.J. *et al.* (2021) RNA editing enzyme APOBEC3A promotes pro-inflammatory M1 macrophage polarization. *Commun Biol*, **4**, 102.

72. Sharma, S., Wang, J., Alqassim, E., Portwood, S., Cortes Gomez, E., Maguire, O., Basse, P.H., Wang, E.S., Segal, B.H. and Baysal, B.E. (2019) Mitochondrial hypoxic stress induces widespread RNA editing by APOBEC3G in natural killer cells. *Genome Biol*, **20**, 37.

73. Alonso de la Vega, A., Temiz, N.A., Tasakis, R., Somogyi, K., Salgueiro, L., Zimmer, E., Ramos, M., Diaz-Jimenez, A., Chocarro, S., Fernandez-Vaquero, M. *et al.* (2023) Acute expression of human APOBEC3B in mice results in RNA editing and lethality. *Genome*

Biol, **24**, 267.

74. Fixman, B., Diaz-Gay, M., Qiu, C., Margaryan, T., Lee, B. and Chen, X.S. (2024) Validation of the APOBEC3A-mediated RNA single base substitution signature and proposal of novel APOBEC1, APOBEC3B, and APOBEC3G RNA signatures. *J Mol Biol*, **436**, 168854.
75. Zhang, C., Lu, Y.J., Wang, M., Chen, B., Xiong, F., Mitsopoulos, C., Rossanese, O., Li, X. and Clarke, P.A. (2024) Characterisation of APOBEC3B-Mediated RNA editing in breast cancer cells reveals regulatory roles of NEAT1 and MALAT1 lncRNAs. *Oncogene*, **43**, 3366-3377.
76. Starrett, G.J., Luengas, E.M., McCann, J.L., Ebrahimi, D., Temiz, N.A., Love, R.P., Feng, Y., Adolph, M.B., Chelico, L., Law, E.K. *et al.* (2016) The DNA cytosine deaminase APOBEC3H haplotype I likely contributes to breast and lung cancer mutagenesis. *Nat Commun*, **7**, 12918.
77. OhAinle, M., Kerns, J.A., Li, M.M., Malik, H.S. and Emerman, M. (2008) Antiretroelement activity of APOBEC3H was lost twice in recent human evolution. *Cell Host Microbe*, **4**, 249-259.
78. Lellek, H., Kirsten, R., Diehl, I., Apostel, F., Buck, F. and Greeve, J. (2000) Purification and molecular cloning of a novel essential component of the apolipoprotein B mRNA editing enzyme-complex. *J Biol Chem*, **275**, 19848-19856.
79. Blanc, V., Xie, Y., Kennedy, S., Riordan, J.D., Rubin, D.C., Madison, B.B., Mills, J.C., Nadeau, J.H. and Davidson, N.O. (2019) Apobec1 complementation factor (A1CF) and RBM47 interact in tissue-specific regulation of C to U RNA editing in mouse intestine and liver. *RNA*, **25**, 70-81.
80. Wolfe, A.D., Arnold, D.B. and Chen, X.S. (2019) Comparison of RNA editing activity of APOBEC1-A1CF and APOBEC1-RBM47 complexes reconstituted in HEK293T cells. *J Mol Biol*, **431**, 1506-1517.
81. Cheng, A.Z., Moraes, S.N., Attarian, C., Yockteng-Melgar, J., Jarvis, M.C., Biolatti, M.,

Galitska, G., Dell'Oste, V., Frappier, L., Bierle, C.J. *et al.* (2019) A conserved mechanism of APOBEC3 relocalization by herpesviral ribonucleotide reductase large subunits. *J Virol*, **93**.

82. Shaban, N.M., Yan, R., Shi, K., Moraes, S.N., Cheng, A.Z., Carpenter, M.A., McLellan, J.S., Yu, Z. and Harris, R.S. (2022) Cryo-EM structure of the EBV ribonucleotide reductase BORF2 and mechanism of APOBEC3B inhibition. *Sci Adv*, **8**, eabm2827.
83. Liu, Z., Chen, S., Lai, L. and Li, Z. (2022) Inhibition of base editors with anti-deaminases derived from viruses. *Nat Commun*, **13**, 597.
84. Grillo, M.J., Jones, K.F.M., Carpenter, M.A., Harris, R.S. and Harki, D.A. (2022) The current toolbox for APOBEC drug discovery. *Trends in Pharmacological Sciences*, **43**, 362-377.
85. Taylor, B.J., Nik-Zainal, S., Wu, Y.L., Stebbings, L.A., Raine, K., Campbell, P.J., Rada, C., Stratton, M.R. and Neuberger, M.S. (2013) DNA deaminases induce break-associated mutation showers with implication of APOBEC3B and 3A in breast cancer kataegis. *Elife*, **2**, e00534.
86. Osgood, N.R.B., Zawalick, N.M., Sawyer, C.B., Cowan, Q.T., Gu, S., Mawson, S.J., Ranzau, B.L., Li, L., Gymrek, M., Goren, A. *et al.* (2025) Genome editing with programmable base editors in human cells. *Methods Enzymol*, **712**, 351-404.